

SN 2011fe: A Laboratory for Testing Models of Type Ia Supernovae

Laura Chomiuk^{A,B,C}

^A Department of Physics and Astronomy, Michigan State University, East Lansing, MI 48824

^B National Radio Astronomy Observatory, P.O. Box O, Socorro, NM 87801

^C Email: chomiuk@pa.msu.edu

Abstract: SN 2011fe is the nearest supernova of Type Ia (SN Ia) discovered in the modern multi-wavelength telescope era, and it also represents the earliest discovery of a SN Ia to date. As a normal SN Ia, SN 2011fe provides an excellent opportunity to decipher long-standing puzzles about the nature of SNe Ia. In this review, we summarize the extensive suite of panchromatic data on SN 2011fe, and gather interpretations of these data to answer four key questions: 1) What explodes in a SN Ia? 2) How does it explode? 3) What is the progenitor of SN 2011fe? and 4) How accurate are SNe Ia as standardizable candles? Most aspects of SN 2011fe are consistent with the canonical picture of a massive CO white dwarf undergoing a deflagration-to-detonation transition. However, there is minimal evidence for a non-degenerate companion star, so SN 2011fe may have marked the merger of two white dwarfs.

Keywords: supernovae: general — supernovae: individual (SN 2011fe) — white dwarfs — novae, cataclysmic variables

1 Introduction

Discovered on 2011 August 24 by the Palomar Transient Factory, SN 2011fe¹ was announced as a Type Ia supernova (SN Ia) remarkably soon after explosion (just 31 hours; Nugent et al. 2011a,b). SN 2011fe is nearby, located in the well-studied galaxy M101 at a distance of ~ 7 Mpc (Figure 1; Shappee & Stanek 2011; Lee & Jang 2012). As the earliest and nearest SN Ia discovered in the modern multi-wavelength telescope era, SN 2011fe presents a unique opportunity to test models and seek answers to long-standing questions about SNe Ia.

Such a testbed has been sorely needed. SNe Ia are widely used by cosmologists to measure the expansion parameters of the Universe, and led to the Nobel Prize-winning discovery of dark energy (Riess et al. 1998; Perlmutter et al. 1999). However, important unknowns remain that stymie the use of SNe Ia as precise cosmological tools. The progenitor systems of SNe Ia are poorly understood, and the explosion mechanism itself is elusive (reviews by Hillebrandt & Niemeyer 2000; Livio 2001; Howell 2011; Wang & Han 2012 contain more details).

This paper reviews the significant body of work already published on SN 2011fe as of mid-2013. I focus on five questions: (i) Is SN 2011fe a normal SN Ia? (ii) What exploded in SN 2011fe? (iii) How did it explode? (iv) What is the progenitor of SN 2011fe? and (v) How accurately can we use SNe Ia as standard candles? A concise summary follows in Section 6.

2 SN 2011fe: A normal SN Ia

The multi-band light curve of SN 2011fe, measured in exquisite detail at UV through IR wavelengths, is typical of SNe Ia (Figure 2; Vinkó et al. 2012; Brown et al. 2012; Richmond & Smith 2012; Munari et al. 2013; Pereira et al. 2013). In the B -band, the light curve declines by $\Delta m_{15} = 1.1$ mag in 15 days (Richmond & Smith 2012; Pereira et al. 2013). To power the light curve of SN 2011fe, $\sim 0.5 M_{\odot}$ of ^{56}Ni is required (Nugent et al. 2011b; Bloom et al. 2012; Pereira et al. 2013). This ^{56}Ni mass is quite typical for SNe Ia (Howell et al. 2009).

In addition, time-resolved optical spectroscopy shows SN 2011fe to be a spectroscopically-normal SN Ia (Parrent et al. 2012; Pereira et al. 2013; Mazzali et al. 2013). SN 2011fe can be classified as “core normal” in the schemes of Benetti et al. (2005) and Branch et al. (2006).

In all relevant details, SN 2011fe appears to be a normal SN Ia. It has, therefore, been taken to be representative of its class. Conclusions reached for SN 2011fe may be extrapolated to SNe Ia generally, but we must be careful in this extrapolation, remembering that SN 2011fe is only one object. A number of recent studies have shown that SNe Ia are diverse, and that differences in their observational properties may imply real variety in progenitor systems and explosion mechanisms (e.g., Foley et al. 2012; Wang et al. 2013).

3 What exploded in SN 2011fe?

While it has long been thought that a SN Ia marks the complete disruption of a white dwarf (e.g., Hoyle &

¹The source was originally dubbed PTF 11kly.

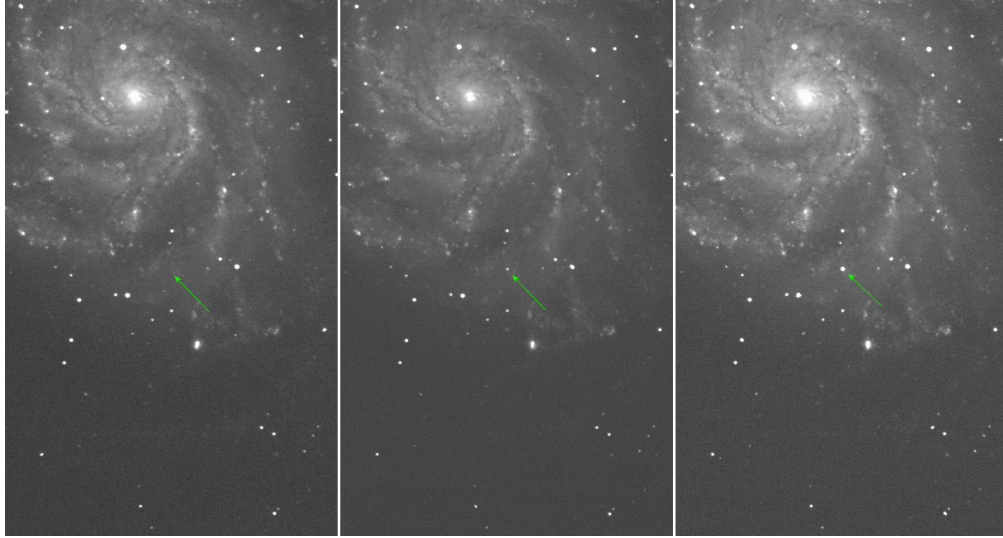


Figure 1: Images of M101 obtained on three successive nights, from left to right: 2011 Aug 23.2, Aug 24.2, and Aug 25.2 UT. The green arrow points to SN 2011fe, which was not detected in the first image but subsequently brightened dramatically. Figure from Nugent et al. (2011b), reprinted by permission from Macmillan Publishers Ltd: Nature, copyright 2011.

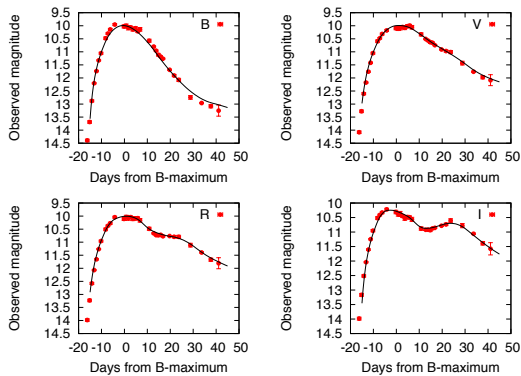


Figure 2: *BVRI* Light curves for SN 2011fe measured in the Johnson-Cousins system (Vega magnitudes). Best-fit SN Ia templates from SALT2 are plotted as black lines. Figure from Vinkó et al. (2012), reproduced with permission ©ESO.

Fowler 1960), little direct proof existed until SN 2011fe.

3.1 Radius of the exploded star

The radius of an exploding star (R_*) can be estimated through the phenomenon of shock breakout: when the SN shock emerges from the surface of the star, it produces a distinctive photometric signature. Shock breakout is expected to appear as an early-time excess in the light curve, with the luminosity and duration of the excess scaling with the radius of the exploding star (Rabinak & Waxman 2011; Kasen 2010; Piro et al. 2010).

The shock breakout constraint depends crucially

on knowing the precise time of the explosion. This is estimated to be UT 2011 August 23 16:29 \pm 20 minutes by Nugent et al. (2011b). They derive this time by fitting a power law to the early optical light curve, following the expectation that the SN luminosity L will increase as the area of the optically-thick photosphere, producing the relation $L \propto t^2$. This simple model fits the photometry very well over the first four days (see Figures 3 and 4).

The modeling of the shock breakout is aided by the serendipitous availability of optical imaging of M101 that had been obtained a mere four hours after Nugent et al.’s estimated time of explosion, but before the SN was actually discovered (Bloom et al. 2012). These data, obtained with The Open University’s 0.4-m telescope, yield a robust non-detection at this epoch. The first detection of SN 2011fe was made 11 hours after Nugent et al.’s estimated explosion time.

The faint optical flux at very early times places strong constraints on the shock breakout signal, implying that the exploding star was compact, with a radius $R_* \lesssim 0.02 R_\odot$ (Figure 3). From the measured ^{56}Ni mass, we know the star was $\gtrsim 0.5 M_\odot$. Only degenerate stars satisfy these mass and radius constraints. Thus the exploded body in SN 2011fe must have been a neutron star or white dwarf. There are no plausible mechanisms for producing SN Ia-like thermonuclear yields from a neutron star (e.g., Jaikumar et al. 2007). Radius constraints therefore provide strong evidence that SN 2011fe marked the explosion of a white dwarf (Bloom et al. 2012).

Several recent papers suggest that this initial analysis may be too simplistic (Piro 2012; Piro & Nakar 2012, 2013; Mazzali et al. 2013). Since the bolometric luminosity of a SN Ia is powered by ^{56}Ni at early times, if the ^{56}Ni is not mixed into the outermost regions of

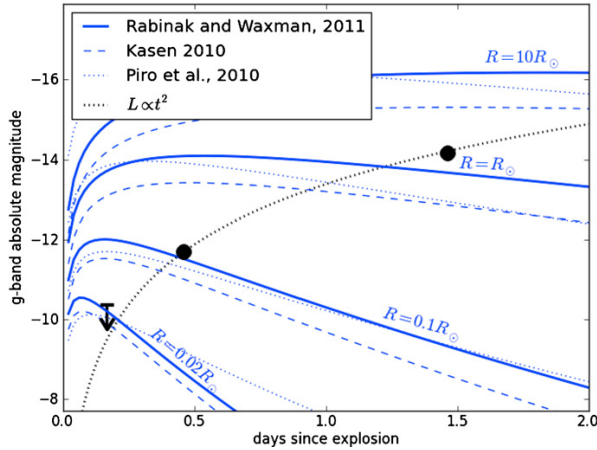


Figure 3: Early-time optical light curve for SN 2011fe plotted as black dots. The light curve is well fit with a simple $L \propto t^2$ power law (dotted black line). Three variations of shock breakout models are plotted as blue lines (Rabinak & Waxman 2011; Kasen 2010; Piro et al. 2010), and are shown for different radii of the exploding star. Assuming that the explosion time can be determined from the simple power-law fit (Nugent et al. 2011b), the non-detection was obtained four hours after explosion and implies a size $R_{\star} \lesssim 0.02 R_{\odot}$ for the exploding star. Figure from Bloom et al. (2012), reproduced by permission of the AAS.

the ejecta, it will take some time for light to diffuse out. The diffusion time could lead to a “dark phase” between explosion and optical rise, lasting a few hours to days depending on the radial profile of ^{56}Ni (Piro & Nakar 2012, 2013).

Supplementing light curves with spectroscopic information about the velocity evolution of the photosphere can help account for this effect. Piro & Nakar (2012) use spectroscopic measurements from Parrent et al. (2012) to refine the explosion date of SN 2011fe backward to UT 2011 August 23 02:30 (with a conservative uncertainty of 0.5 day). This explosion time is 14 hours earlier than that of Nugent et al. (2011b). Using a different spectroscopic data set and modeling strategy, Mazzali et al. (2013) find an explosion time that is more than 33 hours before Nugent et al.’s estimate: UT 2011 August 22 07:00.

These results highlight the uncertainties in constraining the radius of the exploded star with shock breakout models. An earlier explosion time and longer dark phase translate into less stringent radius limits from early-time non-detections (Figure 4). If SN 2011fe has a 24-hour long dark phase, then the photometry presented by Bloom et al. (2012) only limits R_{\star} to $\lesssim 0.1 R_{\odot}$ (Piro & Nakar 2012). As illustrated in Figure 3 of Bloom et al. (2012), this less stringent limit could accommodate unusual non-degenerate stars, such as carbon or perhaps helium stars, as the

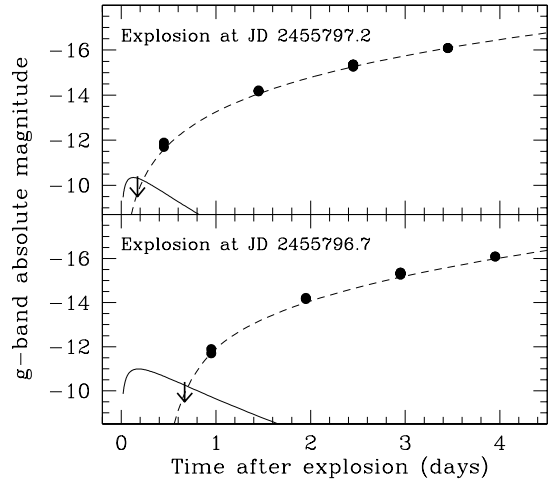


Figure 4: The limits on a shock breakout signature and R_{\star} depend on the estimated explosion date. In both panels, the measured early-time light curve of SN 2011fe is shown as filled circles and an upper-limit arrow. The shock breakout signature is a solid black line, and the SN light curve, powered by ^{56}Ni , is a dashed line. The top panel shows the model of Bloom et al. (2012, as in Figure 3), assuming an explosion date of UT 2011 August 23 16:30 and constraining $R_{\star} \lesssim 0.02 R_{\odot}$. The bottom panel is for an explosion date of UT 2011 August 23 4:30, yielding a 12-hour long dark phase and a larger radius constraint $R_{\star} \lesssim 0.04 R_{\odot}$. Figure from Piro & Nakar (2012), reproduced by permission of the authors.

exploded star in SN 2011fe.

3.2 Abundances in the exploded star

Early-time optical spectra show significant carbon and oxygen features at a range of velocities (7 000–30 000 km s^{-1}) (Nugent et al. 2011b; Parrent et al. 2012; Pereira et al. 2013; Mazzali et al. 2013). Neutral carbon is also observed in IR spectra (Hsiao et al. 2013). SN 2011fe is certainly not alone amongst SNe Ia in showing carbon in its spectrum, although it is the best-studied example. In recent years, a rash of studies have found C II in many SNe Ia spectra, provided that observations are obtained early in the explosion (e.g., Parrent et al. 2011; Folatelli et al. 2012; Silverman & Filippenko 2012). Nugent et al. (2011b) and Parrent et al. (2012) interpret the presence of C in early-time spectra of SN 2011fe as evidence that carbon and oxygen are the unburnt remains of the exploded star. They conclude that the star that exploded as SN 2011fe was likely a CO white dwarf, as commonly expected for SNe Ia (e.g., Livio 2001).

Mazzali et al. (2013) use observations of the fastest-moving outermost layer of ejecta ($v > 19\,400 \text{ km s}^{-1}$) in SN 2011fe to estimate the metallicity of

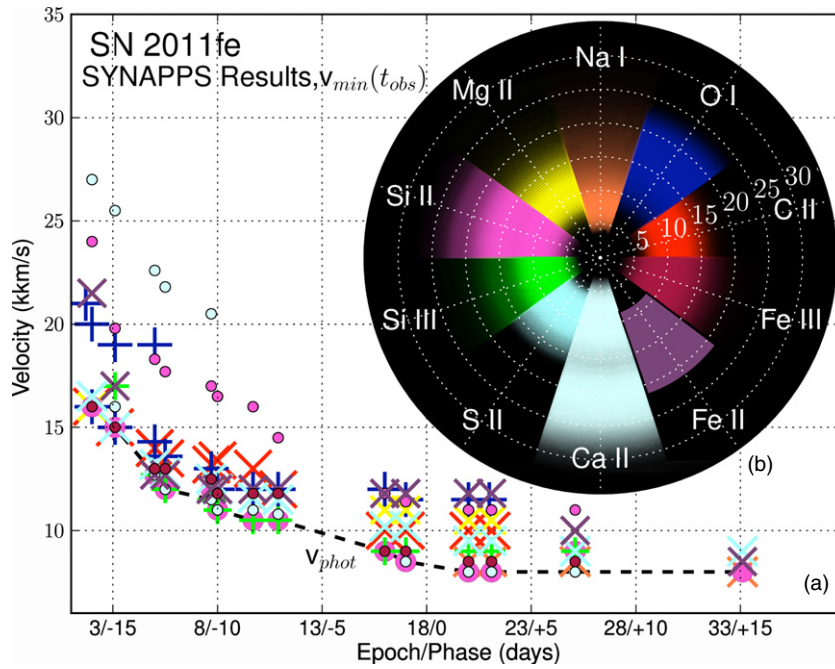


Figure 5: The distribution of ions in the ejecta of SN 2011fe. The larger background panel (a) plots the minimum velocity measured for a given ion as a function of time. Points are color-coded to different ions as shown in the round panel (b). Panel (b) shows the velocity range observed for dominant ions. The circular white dotted lines mark radial increments of $5\,000 \text{ km s}^{-1}$, spanning ejecta velocities of 0 to $30\,000 \text{ km s}^{-1}$. Figure from Parrent et al. (2012), reproduced by permission of the AAS.

the progenitor. Most of this material is carbon, but the remaining 2% of the mass should represent the heavier elements in the progenitor white dwarf. By modeling an Fe-group absorption feature at $\sim 4800 \text{ \AA}$ in conjunction with *HST* UV spectroscopy, Mazzali et al. find a metallicity of $\sim 0.25\text{--}0.5 Z_{\odot}$ for the outermost ejecta. Foley & Kirshner (2013) also use UV spectroscopy to argue that the progenitor of SN 2011fe had sub-solar metallicity. M101’s gas-phase metallicity, measured at the galactocentric radius of SN 2011fe, is $\sim 0.5 Z_{\odot}$ (Stoll et al. 2011)—consistent with estimates for SN 2011fe’s progenitor system. However, it is important to keep in mind that SNe Ia show a range of delays between the formation of the progenitor system and explosion (Maoz & Mannucci 2012); it would not be surprising if there was an offset between the metallicity of SN 2011fe and the current gas-phase metallicity in the region.

The metallicity of the progenitor may be important in shaping a SN Ia, perhaps affecting the yield of ^{56}Ni (Timmes et al. 2003; Jackson et al. 2010) and also determining the observed spectral energy distribution in the rest-frame UV, where high-redshift observations of SNe Ia commonly take place (e.g., Höflich et al. 1998; Lentz et al. 2000; Maguire et al. 2012). The measurements in SN 2011fe are an important data point for testing the predicted effects of metallicity on observed SNe Ia.

3.3 Mass of the exploded star

SN Ia models would be strongly constrained if we could determine whether white dwarfs must reach the Chandrasekhar mass to explode, or if sub-Chandrasekhar explosions are common. Unfortunately, estimates of the ejected mass are challenging to achieve at the necessary accuracy (e.g., Mazzali et al. 1997; Stritzinger et al. 2006). Uncertainties of $<15\%$ are needed to distinguish between Chandrasekhar and sub-Chandrasekhar models, an extremely difficult task given the diversity of elements, densities, and ionic states in the ejecta of SNe Ia.

Mazzali et al. (2013) estimate $\sim 1.1 M_{\odot}$ of material is ejected at speeds $>4\,500 \text{ km s}^{-1}$ in SN 2011fe; this determination is a model-dependent lower limit, as it does not account for the slowest moving material. Future work on nebular spectra may lead to a more complete census of the ejecta mass in SN 2011fe (e.g., Stehle et al. 2005). In the meantime, the ^{56}Ni mass places a secure lower limit on the ejecta mass in SN 2011fe, $M_{ej} > 0.5 M_{\odot}$.

4 How did it explode?

The volume and quality of data available on SN 2011fe enable us to explore the details of the white dwarf’s destruction. What is the relative significance of sub-sonic deflagration and super-sonic detonation fronts? Might the explosion have been triggered by a detona-

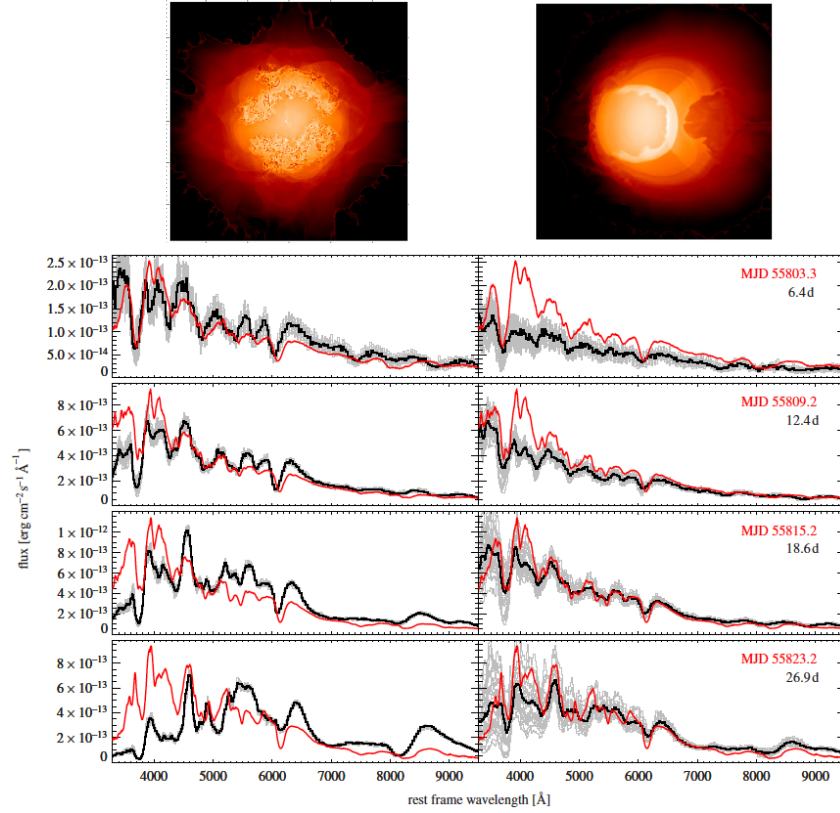


Figure 6: Top-Left Panel: Density distribution of material in a delayed detonation model 100 s after explosion. Top-right panel: Density distribution in a white dwarf merger model 100 s after explosion. Bottom Panels: Optical spectra of SN 2011fe during four epochs spanning 6–27 days after explosion (one epoch per row). Observed spectra are shown in red, and compared with model spectra for the delayed detonation scenario (left column) and the white dwarf merger (right column). Black lines represent models averaged over all viewing angles, while grey lines show model spectra from 25 different viewing angles. Figure from Röpke et al. (2012), reproduced by permission of the AAS.

tion on the white dwarf’s surface? The distribution of newly-synthesized elements within the ejecta can constrain the explosion mechanism of SNe Ia.

Parrent et al. (2012) obtain a time series of optical spectra and fit them using the software package SYNAPPS in order to identify the ions contributing to each spectrum. They measure variations in velocity of each ion’s features with time, and map the velocity range of each ion in Figure 5, ranging from 5 000 to 30 000 km s^{-1} . Figure 5 shows that the ejecta of SN 2011fe are well mixed, with Si, Ca, Fe, and O present throughout much of the ejecta.

As discussed in Section 3.1, the early-time light curve contains information about the radial distribution of newly-synthesized ^{56}Ni . By modeling the light curves and velocity evolution of SN 2011fe, Piro (2012) and Piro & Nakar (2012) find that ^{56}Ni must be present in the outer ejecta, constituting a mass fraction of a few percent at a mass depth of just $10^{-2} M_{\odot}$

below the white dwarf’s surface. Dredge-up of ^{56}Ni to this height may present a challenge to standard delayed detonation models: these posit ignition at many points and result in relatively symmetric explosions. The observed distribution of ^{56}Ni requires strong mixing, as might be provided by an asymmetric deflagration ignition in a delayed detonation scenario (Maeda et al. 2010) or bubbles seen in models of gravitationally confined detonations (Meakin et al. 2009). However, such highly asymmetric models generally conflict with observations of SNe Ia (Blondin et al. 2011) and with spectropolarimetric observations of SN 2011fe (Smith et al. 2011, see below for more discussion). Alternatively, a double detonation scenario (where a He-rich shell detonates on the surface of the white dwarf and drives a shock inward, inducing nuclear burning of the entire white dwarf) might also explain the presence of Fe-group elements at the outer edges of the ejecta (Piro & Nakar 2012). However, double detonation models

also struggle to match the observed spectra of SNe Ia (Kromer et al. 2010; Woosley & Kasen 2011). Recent modeling of the standard delayed-detonation scenario can yield ^{56}Ni at large radii along some lines of sight (?); more work is required to determine if such models can explain the observations of SN 2011fe.

Mazzali et al. (2013) compare a time series of UV+optical spectra with SN Ia explosion models. They consider a pure deflagration model in the form of the famous benchmark W7 (Nomoto et al. 1984), which has a steep density profile at the outermost radii and very little mass expanding at the highest velocities. This model produces good fits to optical spectra, but it overpredicts the flux in the UV—more material is required at large velocity, above the photosphere, in order to absorb this light. The W7 model is contrasted with a delayed detonation model (Iwamoto et al. 1999), which has significantly more material expanding at high velocities ($>16\,000\text{ km s}^{-1}$). However, this model predicts larger blueshifts to the UV Fe-group features than observed. Therefore, Mazzali et al. (2013) compose a hybrid model with an outer density profile of intermediate steepness between the pure-deflagration and delayed detonation models. This hybrid essentially corresponds to a weak delayed detonation and provides a better fit to the optical+UV spectra.

Observations of SN 2011fe are also compared with two different three-dimensional explosion models by Röpke et al. (2012). One model is for a delayed detonation of a Chandrasekhar-mass white dwarf, while the other represents a violent merger of two WDs ($1.1 M_{\odot} + 0.9 M_{\odot}$). Both models produce the right amount of ^{56}Ni to match the light curves of SN 2011fe, and both models can fit the spectra of SN 2011fe reasonably well (Figure 6). The delayed detonation model matches the early time spectra better, while the merger provides a significantly better fit at later times. In both models, the predicted spectra are blue-shifted relative to the data on SN 2011fe; this discrepancy might be resolved by increasing the oxygen-to-carbon ratio in the progenitor white dwarf (assumed in the Röpke et al. study to be 1:1).

Each model of Röpke et al. (2012) provides a range of spectra, varying with viewing angle because the model explosions are not spherically symmetric (grey lines in Figure 6). The merger is significantly more asymmetric than the delayed detonation (top row of Figure 6), so the spectra predicted from the merger model cover a wider swath of possible observations. Future work is needed to test if the relatively asymmetric explosions predicted by white dwarf mergers are inconsistent with spectropolarimetric observations of SNe Ia, which constrain the geometry of the ejecta (Wang & Wheeler 2008).

The spectropolarimetric observations of Smith et al. (2011) find that SN 2011fe is polarized at a level of only $\sim 0.2\text{--}0.4\%$. However, compared with the continuum and other spectral lines, the strong Si $\Pi\lambda 6755$ feature has different time-dependent polarization properties. Smith et al. propose a geometric model wherein the continuum photosphere is an ellipse elongated in the polar direction, with a Si-rich “belt” stretching along the equator. While a unique interpretation of the

spectropolarimetry of SN 2011fe is difficult, the observations hint at some small departures from spherical symmetry.

Most constraints therefore imply that SN 2011fe is consistent with a mildly asymmetric delayed detonation model. In the future, the late-time light curve of SN 2011fe ($\gtrsim 4$ years after explosion) may distinguish between explosion models (Röpke et al. 2012). The amount of radioactive ^{55}Fe in the ejecta (half life: 2.75 yr) scales with the central density of the exploded white dwarf. Therefore, the delayed detonation of a Chandrasekhar-mass white dwarf should be brighter at late times than the merger or two sub-Chandrasekhar white dwarfs. However, it will be challenging to infer the bolometric luminosity solely from optical photometry (McClelland et al. 2013), and the effect of ^{55}Fe will need to be carefully disentangled from the possible late-time contribution of the puffed-up companion star (see Section 5; Shappee et al. 2013a).

5 What is the progenitor of SN 2011fe?

It is generally thought that, in order to explode as a SN Ia, a CO white dwarf must be destabilized by mass transfer from a binary companion. However, the nature of the companion—whether a main sequence, subgiant, or giant star in a “single-degenerate” binary, or another white dwarf in a “double-degenerate” binary—remains unknown. Similar uncertainties exist for the nature of the mass transfer, whether gradual accretion or a sudden merger.

5.1 Constraints on the companion star

Li et al. (2011) study deep pre-explosion *HST* imaging of the site of SN 2011fe in M101. No source is present at the location of SN 2011fe, ruling out bright binary companions like most red giants (Figure 7). These are by far the deepest pre-explosion limits placed on the progenitor of a SN Ia; others have been factors of >60 less sensitive and also yielded non-detections (Maoz & Mannucci 2008). Still, Li et al. cannot exclude main sequence or subgiant companions of $\lesssim 4 M_{\odot}$.

If the SN shock plows over a non-degenerate companion star, this interaction is expected to produce an early-time blue “bump” in the UV/optical light curve (Kasen 2010). The amplitude of this bump depends on the binary separation and viewing angle. Brown et al. (2012) find no such feature in *Swift*/UVOT photometry of SN 2011fe (see also Bloom et al. 2012; Figure 3), and constrain the binary separation to $\sim \text{few} \times 10^{11}\text{ cm}$ ($\sim 0.01\text{ AU}$). This constraint also rules out red giant companions, and, assuming mass transfer by Roche Lobe overflow, it implies a mass of $\lesssim 1 M_{\odot}$ for a potential main sequence companion. However, the dark phase predicted by Piro & Nakar (2012) and discussed in Section 4 may soften these constraints by a factor of several; future work is needed to self-consistently model the dark phase and the ejecta’s interaction with

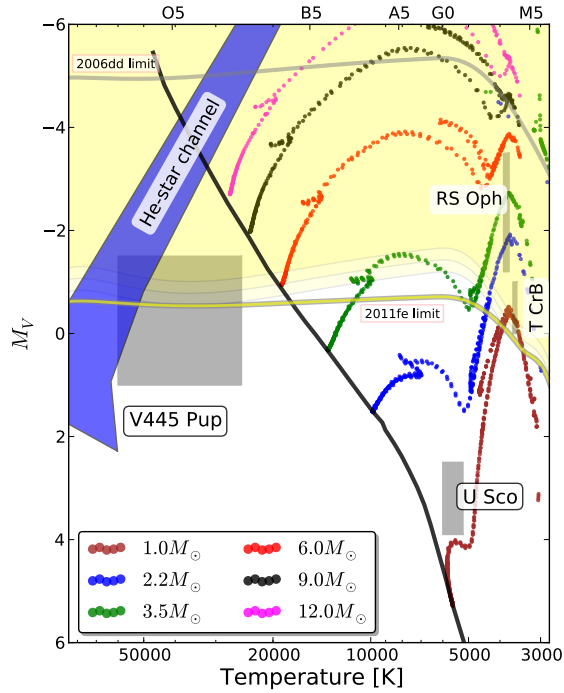


Figure 7: A Hertzsprung-Russell diagram showing the limits on a companion star to SN 2011fe, derived from pre-explosion *HST* imaging. The parameter space above the yellow line is ruled out, excluding most red giants as the companions to SN 2011fe. The stellar main sequence is plotted as a black line and giant branches for stars of various masses are plotted as colored dots (key in bottom left). Several famous candidates for single-degenerate SN Ia progenitors are also plotted as shaded grey regions: recurrent novae with red giant companions (RS Oph and T CrB), a recurrent nova with a main-sequence companion (U Sco), and a He nova (V445 Pup). Figure from Li et al. (2011). Reprinted by permission from Macmillan Publishers Ltd: Nature, copyright 2011.

a companion.

Shappee et al. (2013b) also place constraints on the companion star to SN 2011fe by searching for $H\alpha$ emission in a nebular spectrum nine months after explosion. If the companion to a SN Ia is non-degenerate, $\sim 0.1\text{--}0.2 M_{\odot}$ of hydrogen is predicted to be swept from the companion and entrained in the low-velocity ejecta (Marietta et al. 2000; Pan et al. 2012; Liu et al. 2012b). Once the ejecta become optically thin, the hydrogen-rich material should be observable as $H\alpha$ emission (Mattila et al. 2005). Studies of previous SNe Ia constrained the entrained H to $\lesssim 0.01 M_{\odot}$ (Leonard 2007), but Shappee et al. (2013b) place an order-of-magnitude stronger limit in SN 2011fe, $\lesssim 0.001 M_{\odot}$. If this result holds, it would essentially exclude all non-degenerate secondaries and require a double-degenerate model for SN 2011fe. However, more theoretical work is needed to thoroughly explore gamma-

ray trapping in the ejecta, which is responsible for powering the $H\alpha$ emission. Considerable uncertainties remain in predicting the $H\alpha$ luminosity associated with a given mass of entrained hydrogen, but late-time $H\alpha$ observations hold promise for constraining the companions of SNe Ia.

A final test of the companion to SN 2011fe is possible from late-time observations of the light curve. A non-degenerate companion should expand and grow in luminosity after being shocked by the supernova blast wave; it is expected to remain a factor of $10\text{--}10^3$ over-luminous for $\sim 10^3\text{--}10^4$ yr (Shappee et al. 2013a). The signature of such a puffed-up companion should be visible in SN 2011fe $\gtrsim 3.5$ years after explosion, but could at first be confused with variations in radioactive yields from the SN itself (Röpke et al. 2012). Very late time measurements will effectively search for such an altered companion at the site of SN 2011fe.

5.2 Constraints on the circumbinary medium

A red giant progenitor is also ruled out by searches for circumbinary material using radio and X-ray observations (Horesh et al. 2012; Chomiuk et al. 2012; Margutti et al. 2012). The interaction between a supernova blastwave and the circumstellar medium accelerates particles to relativistic speeds and amplifies the magnetic field in the shock front, producing radio synchrotron emission (Chevalier 1982, 1998). These same relativistic electrons also up-scatter photons radiated by the supernova itself, producing inverse Compton radiation at X-ray wavelengths (Chevalier & Fransson 2006). While these signals are often observed in nearby core-collapse SNe (Weiler et al. 2002; Soderberg et al. 2006), no SN Ia has ever been detected at radio or X-ray wavelengths, implying that SNe Ia do not explode in dense environments (Panagia et al. 2006; Immler et al. 2006; Hancock et al. 2011; Russell & Immler 2012). SN 2011fe is no exception, with multiple epochs of non-detections in deep radio and X-ray data.

With SN 2011fe, we can place the most stringent limits to date on the circumbinary environment around a SN Ia. Assuming the circumbinary material is distributed in a wind profile ($\rho = \frac{\dot{M}}{4\pi v_w r^2}$, where \dot{M} and v_w are the mass-loss rate and velocity of the wind), Chomiuk et al. (2012) use deep radio limits from the Karl G. Jansky Very Large Array to find that $\dot{M} \lesssim 6 \times 10^{-10} M_{\odot} \text{ yr}^{-1}$ in the surroundings of SN 2011fe, for $v_w = 100 \text{ km s}^{-1}$. Assuming a uniform density medium, they find its density must be $n_{\text{CSM}} \lesssim 6 \text{ cm}^{-3}$. These limits on the circumbinary medium not only rule out a red giant companion for SN 2011fe, but also exclude optically-thick accretion winds and non-conservative mass transfer during Roche Lobe overflow (Chomiuk et al. 2012). The environment around SN 2011fe is extremely low-density.

Horesh et al. (2012) caution that radio limits on the circumbinary density depend on poorly-understood microphysical parameters governing the efficiency of particle acceleration and magnetic field amplification. Margutti et al. (2012) use X-ray observations from

Chandra and *Swift* to place constraints on the circumbinary medium which are less model-dependent than the radio limits, because they do not depend on an assumed magnetic field strength. While the X-ray limits on circumbinary density are somewhat less stringent than the radio constraints, it is worth noting that the sensitivity of X-ray observations to circumbinary material scales with the bolometric luminosity of the supernova. The deep *Chandra* observation on SN 2011fe was obtained just three days after discovery, significantly before light curve peak. If instead *Chandra* had observed at optical maximum, the X-ray constraints on circumbinary material around SN 2011fe would be more stringent than the radio limits.

A search for circumbinary dust carried out by Johansson et al. (2013) uses imaging from *Herschel* at 70 μm and 160 μm . Both pre- and post-explosion imaging yield non-detections, constraining the dust mass in the vicinity of SN 2011fe to $\lesssim 7 \times 10^{-3} M_{\odot}$ (assuming a dust temperature of 500 K).

A clean circumbinary environment is also found by Patat et al. (2013), who study optical absorption lines along the line of sight to SN 2011fe. In a few SNe Ia, time-variable Na I D absorption has been observed and attributed to the presence of circumbinary material that is ionized by the SN and then recombines (Patat et al. 2007; Simon et al. 2009). Patat et al. (2013) obtain multi-epoch high-resolution spectroscopy of SN 2011fe and find no evidence for time variability in the Na I D profile, again implying a lack of significant circumbinary material.

5.3 Constraints on the accretion history

The above-described constraints rule out many single-degenerate progenitors, and are often cited as evidence that SN 2011fe was the product of a white dwarf merger. However, the constraints can not conclusively exclude a main-sequence or sub-giant donor of reasonably low mass, $\lesssim 1\text{--}2 M_{\odot}$, transferring material via Roche lobe overflow.

At low mass transfer rates, such a system might look like the recurrent nova U Sco (Figure 7), which ejects $10^{-6} M_{\odot}$ every ~ 10 years in a nova explosion and harbors a white dwarf near the Chandrasekhar mass (Thoroughgood et al. 2001; Diaz et al. 2010; Schaefer 2010; although the white dwarf in U Sco is likely composed of ONe, rather than CO; Mason 2011). Li et al. (2011) collect a time-series of pre-explosion photometry at the site of SN 2011fe to search for novae preceding the supernova. All epochs yield non-detections, and they estimate a $\sim 60\%$ chance that a nova would have been detected if it had erupted in the five years prior to SN 2011fe. There have also been suggestions in the literature that nova shells around SNe Ia should produce time-variable NaD absorption features (Patat et al. 2011); Patat et al. (2013) find no evidence of a nova-like shell surrounding SN 2011fe.

In a progenitor system with a main sequence companion transferring mass at higher rates, steady burning of hydrogen is expected on the white dwarf surface, instead of unstable burning in the form of no-

vae. The white dwarf will radiate thermal emission of $\sim \text{few} \times 10^5$ K, with a spectral energy distribution peaking in the far-UV to soft X-ray. Liu et al. (2012a) and Nielsen et al. (2012) search deep pre-explosion X-ray imaging of the site of SN 2011fe, looking for evidence of such a super-soft X-ray source, and emerge with non-detections. While this constraint rules out many known super-soft sources, it is not stringent enough to exclude those with lower luminosities or cooler temperatures; for example, a source like the persistent super-soft source Cal 83 remains viable (Liu et al. 2012a).

One piece of evidence suggesting a single-degenerate system is that the fastest-moving ejecta ($> 19\,400 \text{ km s}^{-1}$) in SN 2011fe are almost exclusively composed of carbon (98% by mass; Mazzali et al. 2013). Mazzali et al. interpret these outermost ejecta as the ashes of the material accreted onto the white dwarf before the SN. If SN 2011fe marked the merger of two CO white dwarfs, a significant fraction of this material should be oxygen—but the O I feature at 7774 Å. They conclude that the dominance of C in highest-velocity ejecta is support for H-rich accretion onto the white dwarf, because H will fuse to C on the outskirts of a SN Ia, but the ejecta will expand before significant amounts of C can subsequently fuse to O. The outer ejecta might also be consistent with the accretion of helium under special circumstances, but in most conditions He should burn explosively up to the Fe-peak.

A relatively exotic strategy for “hiding” the non-degenerate companion of a SN Ia was proposed by Justham (2011) and Di Stefano et al. (2011) and dubbed the “spin-up/spin-down” model. A white dwarf accreting from a non-degenerate companion may reach significant rotational speeds by conservation of angular momentum, and centripetal force will help support the white dwarf and prevent it from exploding as a SN Ia. Upon the cessation of mass transfer (presumably due to the evolution of the companion), the white dwarf will begin to spin down, and after a delay, it will finally explode as a SN Ia. The spin-down time is uncertain and potentially highly variable, $\sim 10^3\text{--}10^{10}$ yr. This delay may provide sufficient time for the evolved companion to lose any remaining H-rich envelope and contract to a small and unobtrusive radius. While this model can reconcile SN 2011fe to a range of single-degenerate progenitor systems (Hachisu et al. 2012), it is highly speculative. Accreting white dwarfs are observed to spin at significantly lower rates than predicted by simple conservation of momentum (Sion 1999), and the models of spinning white dwarfs remain preliminary (e.g., Yoon & Langer 2005).

6 How accurate are SNe Ia as standardizeable candles?

Because the distance to M101 is relatively well known and because SN 2011fe is so well-studied, it constitutes a test of SNe Ia as standardizeable candles. Matheson et al. (2012) collect distance measurements

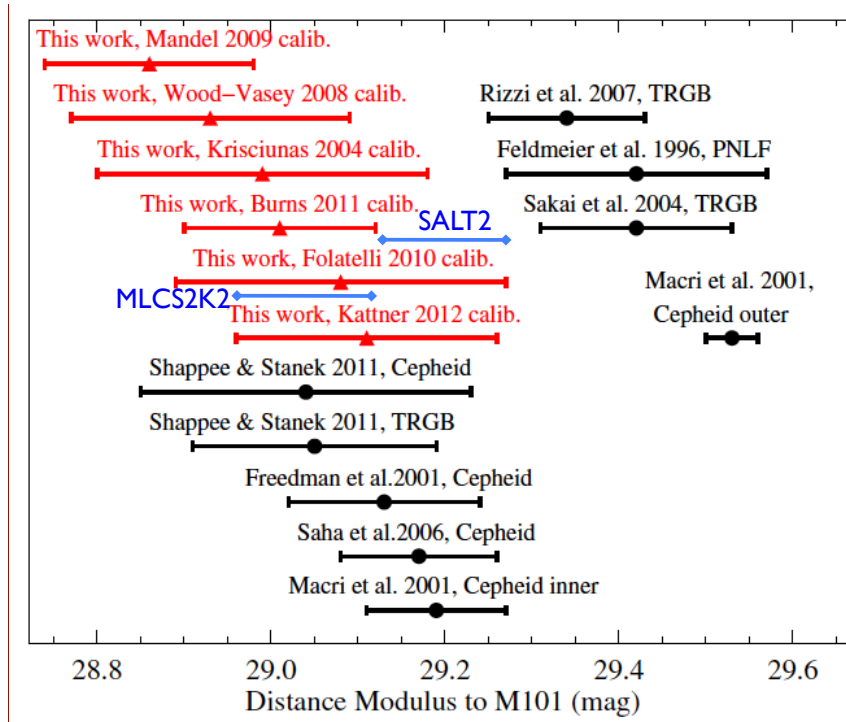


Figure 8: Distance moduli measured to M101 with a range of techniques and 1σ error bars. Black lines are pre-SN 2011fe estimates which use Cepheids, TRGB, or PNLF methods. Red lines use near-IR light curves of SN 2011fe to estimate the distance, and represent fits to a variety of calibrations (Matheson et al. 2012). Blue lines use *BVR* light curves of SN 2011fe with the fitters SALT2 and MLCS2k2 (Vinkó et al. 2012). Figure modified from Matheson et al. (2012) to include data from Vinkó et al. (2012); reproduced by permission of the AAS.

to M101 obtained independent of SN 2011fe, using Cepheid variable stars (Freedman et al. 2001; Macri et al. 2001; Saha et al. 2006; Shappee & Stanek 2011), the tip of the red giant branch (TRGB; Sakai et al. 2004; Rizzi et al. 2007; Shappee & Stanek 2011; also Lee & Jang 2012), and the planetary nebula luminosity function (PNLF; Feldmeier et al. 1996). These estimates span distance moduli of 29.04–29.53 (Figure 8) with a standard deviation of 0.18 mag.

The light curves of SN 2011fe can be used to independently estimate the distance to its host galaxy. Vinkó et al. (2012) observe optical light curves in *BVR* and apply two often-used light curve fitters to estimate the distance to SN 2011fe: MLCS2k2 (Jha et al. 2007) and SALT2 (Figure 2; Guy et al. 2007, 2010). The best-fit MLCS2k2 template returns a distance modulus of 29.21 ± 0.07 mag, while SALT2 yields 29.05 ± 0.08 mag (Figure 8); both assume $H_0 = 73 \text{ km s}^{-1} \text{ Mpc}^{-1}$. The errors in distance moduli are dominated by degeneracies in the template fits, not by noise in the data. The difference in distance modulus measured from these two calibrations is consistent with the scatter in each calibration measured from a larger sample of SNe Ia (~ 0.15 mag; Kessler et al. 2009).

The scatter observed between SN Ia light curves is smaller in the near-IR than in the optical (Phillips 2012). Therefore, Matheson et al. (2012) carry out a

similar procedure as Vinkó et al. (2012), but use *JHK_s* light curves of SN 2011fe to compare various SN Ia calibrations. Plotted in red in Figure 8 are distance moduli calculated using the *H*-band peak apparent brightness of SN 2011fe and six different calibrations of near-IR light curves (Krisciunas et al. 2004; Wood-Vasey et al. 2008; Mandel et al. 2009; Folatelli et al. 2010; Burns et al. 2011; Kattner et al. 2012; assuming $H_0 = 72 \text{ km s}^{-1} \text{ Mpc}^{-1}$). The calibrations yield distance moduli ranging from 28.93 mag to 29.17 mag. Each measurement has a significant uncertainty associated with it, ~ 0.16 mag, due to the scatter in the data used to develop the calibration. The distribution of distance moduli calculated from these calibrations has a standard deviation of 0.12 mag, consistent with the error in a single calibration.

Vinkó et al. (2012) estimate that the error on the distance to M101, using estimates from both Cepheids and SN 2011fe, remains at $\sim 8\%$ —a rather large uncertainty, given that M101 is one of the best-studied nearby galaxies. Still, distance estimates to SN 2011fe agree with recent Cepheid and TRGB distance determinations to M101 within 1σ of quoted systematic errors on these calibrations. These results imply that the systematic errors in standard candle calibrations are well-estimated and large offsets do not exist in zero points.

7 Conclusions

- **What exploded in SN 2011fe?** A carbon/oxygen white dwarf of sub-solar metallicity.
- **How did it explode?** Most data are consistent with a slightly asymmetric delayed detonation, but other scenarios might also fit, if studied in more detail.
- **What is the progenitor of SN 2011fe?** Despite much deeper searches than in any preceding SN Ia, very little evidence for a non-degenerate companion is found in SN 2011fe. Small corners of single-degenerate parameter space remain viable, but the data imply that SN 2011fe may have been the merger of two white dwarfs. It is important to remember that SN 2011fe is just one supernova, and the class of SNe Ia may be diverse.
- **How accurate are SNe Ia as standardizable candles?** Different calibrations of SN Ia light curves, when applied to SN 2011fe, yield a range of distances to M101 with a standard deviation of 11%. These agree with Cepheid and TRGB distances to M101 at the 1σ level.

Because of its early discovery, proximity, and normalcy, SN 2011fe constitutes a unique opportunity for detailed study of a SN Ia. It is likely to be a decade or more before the next similarly bright and nearby SN Ia explodes, and in the meantime theorists should continue to develop models and revisit the exquisite data collected for SN 2011fe, with the goal of further constraining its progenitor system and explosion mechanism. For example, additional work is needed to accurately predict the $H\alpha$ luminosity expected from a single-degenerate SN Ia in the nebular phase. Spectra of SN 2011fe, spanning just one day after explosion to the late nebular phase and the UV to the IR, are a rich observational resource which have just begun to be tapped. Papers modeling the spectra have, to date, considered only a small handful of specific explosion models; future work should more thoroughly explore the parameter space of plausible explosion mechanisms, analyze the uniqueness of predicted observables from different models, and consider all observables when comparing with models.

Late-time photometry on SN 2011fe should be pursued for years to come, with goals of constraining yields of radioactive isotopes and searching for a puffed-up companion star.

Continued efforts to compare observations of SN 2011fe with theory will ensure a solid groundwork for interpreting the large samples of SNe Ia to be obtained with LSST. When the next nearby bright SN Ia explodes, we will be in an even better position to test models of SNe Ia, armed with the next generation of time-domain telescopes like LSST, ASKAP, and LOFT and a polished theoretical framework.

Acknowledgments

L. C. is a Jansky Fellow of the National Radio Astronomy Observatory. She thanks the organizers of the “Supernovae Illuminating the Universe: From Indi-

viduals to Populations” Conference, which took place September 2012 in Garching, Germany. Their kind invitation for a review talk on SN 2011fe was the inspiration for this article. She is also grateful to Ken Shen, Fernando Patat, Alicia Soderberg, Max Moe, and Dean Townsley for helpful discussions, Stuart Ryder and Bryan Gaensler for their patience and work, and an anonymous referee for useful comments.

References

- Benetti, S., et al. 2005, *ApJ*, 623, 1011
- Blondin, S., Kasen, D., Röpke, F. K., Kirshner, R. P., & Mandel, K. S. 2011, *MNRAS*, 417, 1280
- Bloom, J. S., et al. 2012, *ApJ*, 744, L17
- Branch, D., et al. 2006, *PASP*, 118, 560
- Brown, P. J., et al. 2012, *ApJ*, 753, 22
- Burns, C. R., et al. 2011, *AJ*, 141, 19
- Chevalier, R. A. 1982, *ApJ*, 259, 302
- . 1998, *ApJ*, 499, 810
- Chevalier, R. A., & Fransson, C. 2006, *ApJ*, 651, 381
- Chomiuk, L., et al. 2012, *ApJ*, 750, 164
- Di Stefano, R., Voss, R., & Claeys, J. S. W. 2011, *ApJ*, 738, L1
- Diaz, M. P., Williams, R. E., Luna, G. J., Moraes, M., & Takeda, L. 2010, *AJ*, 140, 1860
- Feldmeier, J. J., Ciardullo, R., & Jacoby, G. H. 1996, *ApJ*, 461, L25
- Folatelli, G., et al. 2010, *AJ*, 139, 120
- . 2012, *ApJ*, 745, 74
- Foley, R. J., & Kirshner, R. P. 2013, *ApJ*, 769, L1
- Foley, R. J., et al. 2012, *ApJ*, 752, 101
- Freedman, W. L., et al. 2001, *ApJ*, 553, 47
- Guy, J., et al. 2007, *A&A*, 466, 11
- . 2010, *A&A*, 523, A7
- Hachisu, I., Kato, M., & Nomoto, K. 2012, *ApJ*, 756, L4
- Hancock, P. P., Gaensler, B. M., & Murphy, T. 2011, *ApJ*, 735, L35
- Hillebrandt, W., & Niemeyer, J. C. 2000, *ARAA*, 38, 191
- Höflich, P., Wheeler, J. C., & Thielemann, F. K. 1998, *ApJ*, 495, 617
- Horesh, A., et al. 2012, *ApJ*, 746, 21

- Howell, D. A. 2011, *Nature Communications*, 2
- Howell, D. A., et al. 2009, *ApJ*, 691, 661
- Hoyle, F., & Fowler, W. A. 1960, *ApJ*, 132, 565
- Hsiao, E. Y., et al. 2013, *ApJ*, 766, 72
- Immler, S., et al. 2006, *ApJ*, 648, L119
- Iwamoto, K., Brachwitz, F., Nomoto, K., Kishimoto, N., Umeda, H., Hix, W. R., & Thielemann, F.-K. 1999, *ApJS*, 125, 439
- Jackson, A. P., Calder, A. C., Townsley, D. M., Chamulak, D. A., Brown, E. F., & Timmes, F. X. 2010, *ApJ*, 720, 99
- Jaikumar, P., Meyer, B. S., Otsuki, K., & Ouyed, R. 2007, *A&A*, 471, 227
- Jha, S., Riess, A. G., & Kirshner, R. P. 2007, *ApJ*, 659, 122
- Johansson, J., Amanullah, R., & Goobar, A. 2013, *MNRAS*, 431, L43
- Justham, S. 2011, *ApJ*, 730, L34
- Kasen, D. 2010, *ApJ*, 708, 1025
- Kattner, S., et al. 2012, *PASP*, 124, 114
- Kessler, R., et al. 2009, *ApJS*, 185, 32
- Krisciunas, K., Phillips, M. M., & Suntzeff, N. B. 2004, *ApJ*, 602, L81
- Kromer, M., Sim, S. A., Fink, M., Röpke, F. K., Seitenzahl, I. R., & Hillebrandt, W. 2010, *ApJ*, 719, 1067
- Lee, M. G., & Jang, I. S. 2012, *ApJ*, 760, L14
- Lentz, E. J., Baron, E., Branch, D., Hauschildt, P. H., & Nugent, P. E. 2000, *ApJ*, 530, 966
- Leonard, D. C. 2007, *ApJ*, 670, 1275
- Li, W., et al. 2011, *Nature*, 480, 348
- Liu, J., Di Stefano, R., Wang, T., & Moe, M. 2012a, *ApJ*, 749, 141
- Liu, Z. W., Pakmor, R., Röpke, F. K., Edelmann, P., Wang, B., Kromer, M., Hillebrandt, W., & Han, Z. W. 2012b, *A&A*, 548, A2
- Livio, M. 2001, in *Supernovae and Gamma-Ray Bursts: the Greatest Explosions since the Big Bang*, ed. M. Livio, N. Panagia, & K. Sahu, 334
- Macri, L. M., et al. 2001, *ApJ*, 549, 721
- Maeda, K., Röpke, F. K., Fink, M., Hillebrandt, W., Travaglio, C., & Thielemann, F.-K. 2010, *ApJ*, 712, 624
- Maguire, K., et al. 2012, *MNRAS*, 426, 2359
- Mandel, K. S., Wood-Vasey, W. M., Friedman, A. S., & Kirshner, R. P. 2009, *ApJ*, 704, 629
- Maoz, D., & Mannucci, F. 2008, *MNRAS*, 388, 421
- . 2012, *PASA*, 29, 447
- Margutti, R., et al. 2012, *ApJ*, 751, 134
- Marietta, E., Burrows, A., & Fryxell, B. 2000, *ApJS*, 128, 615
- Mason, E. 2011, *A&A*, 532, L11
- Matheson, T., et al. 2012, *ApJ*, 754, 19
- Mattila, S., Lundqvist, P., Sollerman, J., Kozma, C., Baron, E., Fransson, C., Leibundgut, B., & Nomoto, K. 2005, *A&A*, 443, 649
- Mazzali, P., et al. 2013, arXiv 1305.2356
- Mazzali, P. A., Chugai, N., Turatto, M., Lucy, L. B., Danziger, I. J., Cappellaro, E., della Valle, M., & Benetti, S. 1997, *MNRAS*, 284, 151
- McClelland, C. M., Garnavich, P. M., Milne, P. A., Shappee, B. J., & Pogge, R. W. 2013, *ApJ*, 767, 119
- Meakin, C. A., Seitenzahl, I., Townsley, D., Jordan, IV, G. C., Truran, J., & Lamb, D. 2009, *ApJ*, 693, 1188
- Munari, U., Henden, A., Belligoli, R., Castellani, F., Cherini, G., Righetti, G. L., & Vagnozzi, A. 2013, *NewA*, 20, 30
- Nielsen, M. T. B., Voss, R., & Nelemans, G. 2012, *MNRAS*, 426, 2668
- Nomoto, K., Thielemann, F.-K., & Yokoi, K. 1984, *ApJ*, 286, 644
- Nugent, P., Sullivan, M., Bersier, D., Howell, D. A., Thomas, R., & James, P. 2011a, *ATel*, 3581
- Nugent, P. E., et al. 2011b, *Nature*, 480, 344
- Pan, K.-C., Ricker, P. M., & Taam, R. E. 2012, *ApJ*, 750, 151
- Panagia, N., Van Dyk, S. D., Weiler, K. W., Sramek, R. A., Stockdale, C. J., & Murata, K. P. 2006, *ApJ*, 646, 369
- Parrent, J. T., et al. 2012, *ApJ*, 752, L26
- . 2011, *ApJ*, 732, 30
- Patat, F., et al. 2007, *Science*, 317, 924
- Patat, F., Chugai, N. N., Podsiadlowski, P., Mason, E., Melo, C., & Pasquini, L. 2011, *A&A*, 530, A63
- Patat, F., et al. 2013, *A&A*, 549, A62
- Pereira, R., et al. 2013, arXiv 1302.1292
- Perlmutter, S., et al. 1999, *ApJ*, 517, 565

- Phillips, M. M. 2012, *PASA*, 29, 434
- Piro, A. L. 2012, *ApJ*, 759, 83
- Piro, A. L., Chang, P., & Weinberg, N. N. 2010, *ApJ*, 708, 598
- Piro, A. L., & Nakar, E. 2012, arXiv 1211.6438
- . 2013, *ApJ*, 769, 67
- Rabinak, I., & Waxman, E. 2011, *ApJ*, 728, 63
- Richmond, M. W., & Smith, H. A. 2012, *JAAVSO*, 40, 872
- Riess, A. G., et al. 1998, *AJ*, 116, 1009
- Rizzi, L., Tully, R. B., Makarov, D., Makarova, L., Dolphin, A. E., Sakai, S., & Shaya, E. J. 2007, *ApJ*, 661, 815
- Röpke, F. K., et al. 2012, *ApJ*, 750, L19
- Russell, B. R., & Immler, S. 2012, *ApJ*, 748, L29
- Saha, A., Thim, F., Tammann, G. A., Reindl, B., & Sandage, A. 2006, *ApJS*, 165, 108
- Sakai, S., Ferrarese, L., Kennicutt, Jr., R. C., & Saha, A. 2004, *ApJ*, 608, 42
- Schaefer, B. E. 2010, *ApJS*, 187, 275
- Shappee, B. J., Kochanek, C. S., & Stanek, K. Z. 2013a, *ApJ*, 765, 150
- Shappee, B. J., & Stanek, K. Z. 2011, *ApJ*, 733, 124
- Shappee, B. J., Stanek, K. Z., Pogge, R. W., & Garnavich, P. M. 2013b, *ApJ*, 762, L5
- Silverman, J. M., & Filippenko, A. V. 2012, *MNRAS*, 425, 1917
- Simon, J. D., et al. 2009, *ApJ*, 702, 1157
- Sion, E. M. 1999, *PASP*, 111, 532
- Smith, P. S., Williams, G. G., Smith, N., Milne, P. A., Jannuzi, B. T., & Green, E. M. 2011, arXiv 1111.6626
- Soderberg, A. M., Chevalier, R. A., Kulkarni, S. R., & Frail, D. A. 2006, *ApJ*, 651, 1005
- Stehle, M., Mazzali, P. A., Benetti, S., & Hillebrandt, W. 2005, *MNRAS*, 360, 1231
- Stoll, R., Shappee, B., & Stanek, K. Z. 2011, *ATel*, 3588
- Stritzinger, M., Leibundgut, B., Walch, S., & Conrardo, G. 2006, *A&A*, 450, 241
- Thoroughgood, T. D., Dhillon, V. S., Littlefair, S. P., Marsh, T. R., & Smith, D. A. 2001, *MNRAS*, 327, 1323
- Timmes, F. X., Brown, E. F., & Truran, J. W. 2003, *ApJ*, 590, L83
- Vinkó, J., et al. 2012, *A&A*, 546, A12
- Wang, B., & Han, Z. 2012, *NewAR*, 56, 122
- Wang, L., & Wheeler, J. C. 2008, *ARAA*, 46, 433
- Wang, X., Wang, L., Filippenko, A. V., Zhang, T., & Zhao, X. 2013, *Science*, 340, 170
- Weiler, K. W., Panagia, N., Montes, M. J., & Sramek, R. A. 2002, *ARAA*, 40, 387
- Wood-Vasey, W. M., et al. 2008, *ApJ*, 689, 377
- Woosley, S. E., & Kasen, D. 2011, *ApJ*, 734, 38
- Yoon, S.-C., & Langer, N. 2005, *A&A*, 435, 967